MODEL OF THE PROCESSES OF HEAT, MASS AND CHARGE TRANSFER IN THE ANODE REGION AND COLUMN OF THE WELDING ARC WITH REFRACTORY CATHODE

I.V. KRIVTSUN[1], **V.F. DEMCHENKO**[1] and **I.V. KRIKENT**[2]
[1]E.O. Paton Electric Welding Institute, NASU, Kiev, Ukraine
[2]Dneprodzerzhinsk State Technical University, Dneprodzerzhinsk, Ukraine

The main difference of the proposed mathematical model of the welding arc from the known ones describing the atmospheric-pressure arcs is allowance for the multi-component composition of the arc plasma, which is caused by evaporation of the anode metal and convective diffusion of metal vapours in the arc column. The model can be used for numerical analysis of thermal, gas-dynamic and electromagnetic characteristics of the arc plasma in inert-gas tungsten-electrode and plasma welding, as well as for modelling of thermal and dynamic effects of the arc on the weld pool surface.

Keywords: *tungsten-electrode welding, plasma welding, electric arc, arc column, multi-component plasma, anode region, anode potential drop, mathematical model*

Many models are available for numerical investigation of the processes of energy, impulse, mass and charge transfer in plasma of the electric arc, as well as of the processes of its interaction with electrodes using different arc welding methods [1–14]. However, most of them assume that the arc plasma is one-component, i.e. containing atoms and ions of a shielding or plasma gas, which is the inert one in the majority of cases. As a rule, plasma of the real welding arcs is multi-component, as along with gas particles it also contains atoms and ions of an evaporating material of electrodes, and anode in the first turn. Therefore, it is necessary to allow for the multi-component nature of the arc plasma in development of an adequate mathematical model.

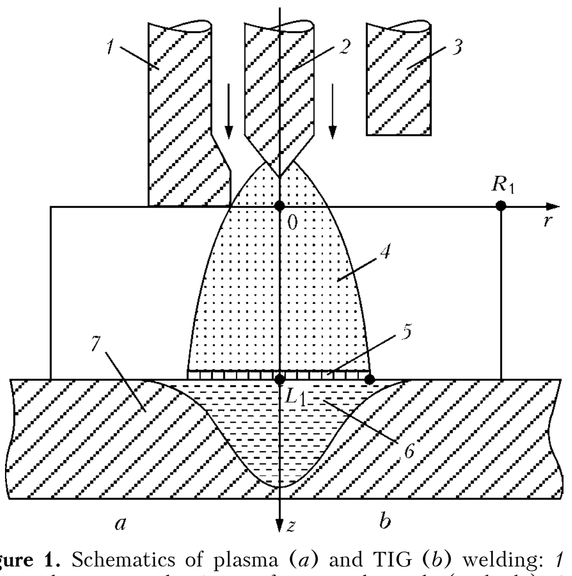

Figure 1. Schematics of plasma (*a*) and TIG (*b*) welding: *1* — plasma-shaping nozzle; *2* — refractory electrode (cathode); *3* — shielding gas nozzle; *4* — arc column; *5* — anode region of the arc; *6* — weld pool; *7* — workpiece (anode)

Such a model must have another important characteristic — self-consistency, which makes it possible to allow for relationship between the physical processes occurring at electrodes and in near-electrode plasma regions and processes occurring in the arc column. It should be noted that the majority of studies dedicated to integrated modelling of the electric (including welding) arc use fairly simplified models of the near-electrode regions [4, 6, 9–12], whereas studies dedicated to investigation of the near-electrode phenomena (e.g. [15] and references given in it) pay an insufficient attention to the processes occurring in the arc column.

As theories of the cathode phenomena, as well as processes occurring in the near-cathode plasma of the electric arc with a refractory (non-evaporating) cathode are adequately elaborated [16–19], the purpose of the present study consists in development of the self-consistent mathematical model of physical processes taking place in the anode region and welding arc column (electric arc with the evaporating anode) in inert-gas tungsten-electrode and plasma welding (Figure 1).

Processes occurring in the arc plasma adjoining the surface of the evaporating anode are described by using the approach suggested in studies [20–22], according to which the near-anode plasma is conditionally subdivided into three zones (Figure 2).

The first zone directly adjoining the anode surface is a layer of the space charge, wherein the condition of quasi-neutrality of the plasma in violated and the main potential drop takes place between the plasma and anode. This layer can be considered collisionless, as under a pressure close to the atmospheric one and at electron temperature T_e ~ 1 eV characteristic of the conditions under investigation [23, 24], thickness of this layer $\bar{x}$ commensurable with Debye radius $r_D \sim$ $\sim 1\cdot10^{-8}$ m (here and further on the line over a letter means that the value relates to the external boundary of the space charge layer) turns out to be much smaller than the characteristic length of free path of the plasma particles, $l \sim 1\cdot10^{-7}$–$1\cdot10^{-5}$ m (estimations in this study were made for the atmospheric-pressure Fe-plasma).

The second zone is an ionisation region of the non-isothermal quasi-neutral plasma (presheath), wherein the charged particles are generated due to plasma electron ionisation of the gas atoms desorbed from the surface of the metallic anode and evaporating metal atoms. Ions formed here are accelerated towards the anode surface by the electric field induced by more mobile electrons and recombine near this surface. Therefore, conditions of local ionisation equilibrium are violated within the ionisation region. Moreover, a marked change of the plasma potential takes place here, which can be commensurable with its drop in the space charge layer.

The Knudsen layer boundary, which we will compare with a boundary of the anode region, is situated at a distance from the anode surface equal to several lengths of free path of the heavy particles. The third zone begins outside the anode region. This zone is a gas-dynamic plasma region with a local thermodynamic equilibrium formed therein. It should be noted that this region can also be conditionally subdivided into two zones: thermal boundary layer, wherein electron and heavy particles temperatures, T_e^0 and T_h^0, level with the plasma temperature in the arc column, T, and the arc column proper [23].

Because Knudsen layer thickness $L_K \sim 1\cdot10^{-4}$ m is much smaller than anode surface (weld pool) curvature radius $R \sim 1\cdot10^{-3}$ m, the latter can be assumed to be flat in description of the processes occurring in the anode region. As L_K is much smaller than the characteristic scale of measurement of plasma parameters in the gas-dynamic region, when considering the transfer processes taking place in the arc column the anode region can be assumed to be infinitely thin. Therefore, from the standpoint of mathematical description of the processes in the arc plasma, it can be broken down into two regions: anode region (or Knudsen layer) and arc column (or gas-dynamic region), for which the first region is a discontinuity surface. In this connection, the self-consistent mathematical model of the processes of energy, mass and charge transfer in the column plasma and anode region of the welding arc with the refractory cathode should include two interrelated models: model of the thermal, electromagnetic, gas-dynamic and diffusion processes occurring in the multi-component plasma of the arc column, and model of the anode region of the arc, which makes it possible to formulate boundary conditions on the anode surface required to solve equations of the arc column model and determine characteristics

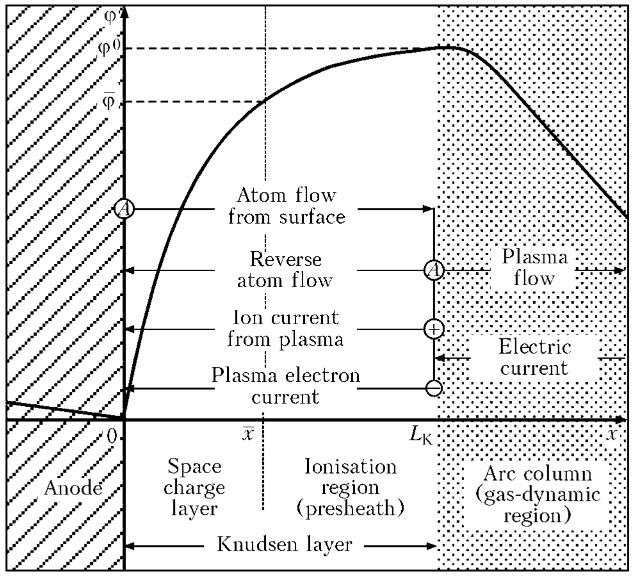

Figure 2. Structure of plasma presheath, particle flows and distribution of potential in the anode region of the welding arc: $\bar{\varphi}$ — value of potential at the space charge boundary layer; A — atoms; + — ions; − — electrons; the rest of the designations are given in the text

of the thermal and dynamic effect of the arc on the weld pool surface.

Consider first the model of the processes of charge, mass and energy transfer in the anode region of the welding arc.

Model of the anode region. To describe processes occurring in the anode region of the arc with the evaporating anode, assume that plasma at the external boundary of this region is characterised by the following parameters: n_e^0 — concentration of electrons; $n_{\alpha Z}^0$ — concentration of atoms (charge number $Z = 0$) and ions ($Z = 1$) of the shielding or plasma gas (kind of particles $\alpha = g$), atoms ($Z = 0$) and ions ($Z = 1$, 2) of the metal vapour ($\alpha = m$); Z_e — ion charge; e — elementary charge; T_h^0 — temperature of heavy particles, which is assumed to be identical for all kinds of atoms and ions, but differing from T_e^0 (two-temperature plasma model); m_e — electron mass; M_α — masses of heavy particles (atoms and ions) of gas ($\alpha = g$) and metal ($\alpha =$ $= m$); and j_a — density of the electric current on the anode surface. As noted above, the anode region can be considered flat. Hence, the n_e^0, $n_{\alpha Z}^0$, T_e^0, T_h^0 and j_a values can be regarded as local, corresponding to a given point on the anode surface, which is characterised by a local value of temperature T_s.

Assume that the current is transferred to the anode only with electrons and ions coming from the plasma (assume that ions arriving on the anode surface recombine there and come back in the form of atoms, and the flow of electrons emitted by the anode is negligibly small). Then the total density of the electric current on the anode surface can be represented as follows:

$$j_a = j_e - j_i \ (j_a > 0), \qquad (1)$$

where j_e is the density of the electric current coming to the anode, and $J_i = \sum_{\alpha = m,\, g;\, Z \geq 1} j_{\alpha Z}$ is the total density of the ion current (for ions of all kinds and charges).

The electron component of the plasma within the anode region can be considered collisionless to a high degree of accuracy, and electron temperature — almost constant through its thickness. In addition, as the plasma potential is, as a rule, higher than the anode potential [24], electrons are decelerated by the electric field, and ions are accelerated towards the anode surface. In this case, the density of the electron current on the anode is [23]

$$j_e = \frac{1}{4} e n_e^0 v_{T_e} \exp\left(-\frac{e\varphi^0}{kT_e^0}\right), \qquad (2)$$

where $v_{T_e} = \sqrt{\frac{8kT_e^0}{\pi m_e}}$ is the thermal velocity of electrons at the external boundary of the anode region; k is the Boltzmann constant; and φ^0 is the plasma potential with respect to the anode surface ($\varphi^0 > 0$).

To find the ion currents, it is necessary to consider the processes occurring in the ionisation region, wherein ions are generated and accelerated towards the anode. For this, we will use the approach [25] based on an assumption that the length of the free path of ions relative to Coulomb collisions between them is much smaller than the ionisation length and length of their free path at collision with atoms (their characteristic values, respectively, are as follows: $l_{ii} \sim 1 \cdot 10^{-7}$ m, $l_{ion} \sim 1 \cdot 10^{-6}$ m, $l_{ia} \sim 1 \cdot 10^{-5}$ m). This suggests that ions in the presheath are intensively maxwellised and acquire the common directed motion velocity, the value of which at a boundary of the ionisation region with the space charge layer is determined by the following expression:

$$\overline{V}_i \equiv v_i(\overline{x}) = \sqrt{\frac{\sum_{\alpha = m,\, g;\, Z \geq 1} k(ZT_e^0 + T_h^0) n_{\alpha Z}^0}{\sum_{\alpha = m,\, g;\, Z \geq 1} M_\alpha n_{\alpha Z}^0}};$$

$$\left(\overline{V}_i = \frac{w^0}{2}\left[\sqrt{1 + \frac{4\sum_{Z \geq 1} k(ZT_e^0 + T_h^0) n_{\alpha Z}^0}{(w^0)^2 \sum_{Z \geq 1} M_m n_{mZ}^0}} - 1\right]\right). \qquad (3)$$

The first relationship in formula (3) corresponds to the diffusion mode of evaporation ($w^0 \approx 0$) [22], whereas the expression in brackets corresponds to the convective mode of evaporation of the anode metal ($w^0 > 0$), where w^0 is the vapour velocity at the anode region boundary, which is normal to the anode surface.

By selecting such a value of $\overline{x}$ as a boundary of the presheath with the space charge layer, at which the plasma quasi-neutrality condition is violated [26], we find the concentration of charged particles at this boundary [22]:

$$\overline{n}_e \equiv n_e(\overline{x}) = n_e^0 \exp\left(-\frac{1}{2}\right);$$
$$\overline{n}_{\alpha Z} \equiv n_{\alpha Z}(\overline{x}) = n_{\alpha Z}^0 \exp\left(-\frac{1}{2}\right), \quad \alpha = m,\, g;\, Z \geq 1. \qquad (4)$$

Then the ion currents to the anode surface can be written down as follows:

$$j_{\alpha Z} = Zen_{\alpha Z}^0 \exp\left(-\frac{1}{2}\right) \overline{V}_i, \quad \alpha = m, \quad g;\, Z \geq 1. \qquad (5)$$

In the convective mode of evaporation of the anode, the exp (−1/2) value in (4) and (5) should be replaced by

$$\exp\left[-\frac{(w^0)^2 \sum_{Z \geq 1} M_m n_{mZ}^0}{8\sum_{Z \geq 1} k(ZT_e^0 + T_h^0) n_{mZ}^0} \times \left\{1 + \sqrt{1 + \frac{4\sum_{Z \geq 1} k(ZT_e^0 + T_h^0) n_{mZ}^0}{(w^0)^2 \sum_{Z \geq 1} M_m n_{mZ}^0}}\right\}^2\right].$$

The values of the electron and ion currents on the anode surface being known, plasma potential φ^0 relative to this surface or anode potential drop U_a can be easily found from equation (1):

$$U_a \equiv -\varphi^0 = -\frac{kT_e^0}{e} \ln\left(\frac{e n_e^0 v_{T_e}}{4\left[j_a + \sum_{\alpha = m,\, g;\, Z \geq 1} j_{\alpha Z}\right]}\right). \qquad (6)$$

Calculation of the j_e, $j_{\alpha Z}$ and U_a values requires the knowledge of temperatures T_e^0 and T_h^0, as well as concentrations n_e^0 and $n_{\alpha Z}^0$ of the charged particles at the external boundary of the anode region. Assuming that the multi-component plasma in the arc column is ionisation-equilibrium, the composition of such plasma at a boundary with the anode region can be determined by using the following system of equations:

- Saha equation allowing for plasma imperfection

$$\frac{n_e^0 n_{\alpha Z+1}^0}{n_{\alpha Z}^0} = \left(\frac{2\pi m_e k T_e^0}{h^2}\right)^{3/2} \frac{2\theta_{\alpha Z+1}}{\theta_{\alpha Z}} \times \exp\left[-\frac{e(U_{\alpha Z} - \Delta U_Z)}{kT_e^0}\right], \quad \alpha = m,\, g; \;\; Z \geq 0, \qquad (7)$$

where h is the Planck's constant; $\theta_{\alpha Z}$ are the statistical sums for heavy particles of kind α, which are in charged state Z; $U_{\alpha Z}$ are the ionisation potentials (for transfer of the particles of kind α from charged state Z to $Z + 1$); $\Delta U_Z = \frac{e(Z + 1)}{r_D}$ is the decrease of the ionisation potentials caused by interaction of the charged particles of the plasma; and

$$r_{\rm D} = \left[kT_e^0/4\pi e^2 \left(n_e^0 + \frac{T_e^0}{T_h^0} \sum_{\alpha = m,\, g;\, Z \ge 1} n_{\alpha Z}^0 Z^{\,2} \right) \right]^{-1/2};$$

• quasi-neutrality condition of plasma

$$n_e^0 = \sum_{\alpha = m,\, g;\, Z \ge 1} n_{\alpha Z}^0 Z; \tag{8}$$

• law of partial pressures

$$p = n_e^0 kT_e^0 + \sum_{Z \ge 0} n_{mZ}^0 kT_h^0 + \sum_{Z \ge 0} n_{gZ}^0 kT_h^0 - \Delta p. \tag{9}$$

Here p is the plasma pressure near the anode, and $\Delta p = \frac{1}{6} \frac{e^2}{r_{\rm D}} \left(n_e^0 + \sum_{\alpha = m,\, g;\, Z \ge 0} n_{\alpha Z}^0 Z^{\,2} \right)$ is the decrease of the pressure due to the plasma imperfection [27].

Another condition determining the concentration of the metal vapour particles at the external boundary of the anode region is required to close the system of equations (7) through (9). With the diffusion mode of evaporation, the rate of diffusion of the vapour particles is assumed to be low, i.e. the vapour state is close to saturation. The equality of partial pressure of the heavy particles of the evaporated metal at this boundary to saturated vapour pressure p_s over the surface of the molten metal with temperature T_s can be chosen as such a condition:

$$\sum_{Z \ge 0} n_{mZ}^0 kT_h^0 = p_s \equiv p_0 \exp \left[\frac{\lambda_v}{k} \left(\frac{1}{T_{\rm B}} - \frac{1}{T_s} \right) \right], \tag{10}$$

where p_0 is the atmospheric pressure; $T_{\rm B}$ is the boiling temperature; λ_v is the work function of the anode metal atom; and $T_h^0 = T_s$.

If the anode surface temperature exceeds the temperature at which the ionised vapour pressure becomes higher than the external pressure ($p_m^0 \equiv n_e^0 kT_e^0 + \sum_{Z \ge 0} n_{mZ}^0 kT_h^0 - \Delta p \ge p$), the vapour starts expanding (spreading), thus pressing away the external gas. As a result, the near-anode plasma becomes one-component, i.e. containing only the evaporated metal particles. It should be noted that metal boiling temperature $T_{\rm B}$ at the absence of ionisation serves as a boundary temperature of the surface, above which the vapour begins spreading into the atmospheric pressure environment (the saturated vapour pressure is equal to the atmospheric one). The impact on this boundary temperature by the electron pressure was investigated in [22]. It follows from the results obtained that the anode surface temperature, above which the ionised vapour pressure becomes higher than the atmospheric one, and the diffusion evaporation mode is replaced by the convective one, becomes much lower than $T_{\rm B}$ with increase in T_e^0.

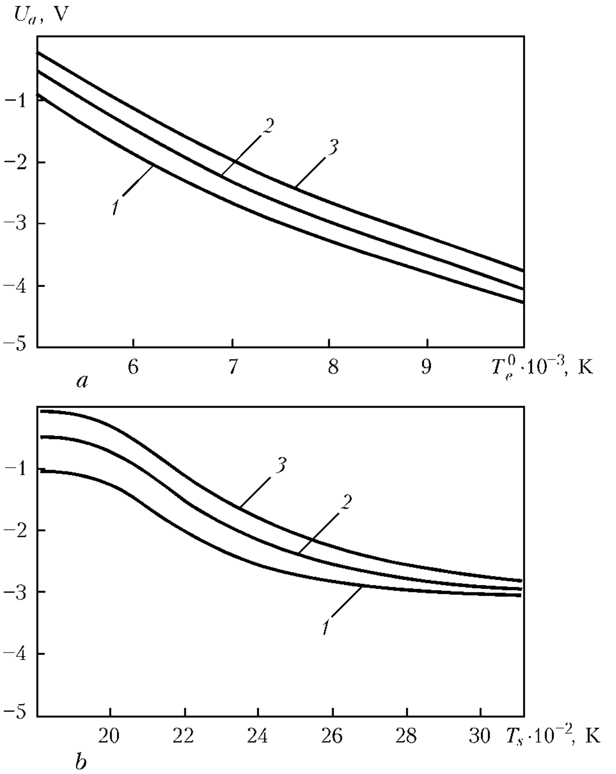

Figure 3. Anode potential drop U_a versus electron temperature in the near-anode plasma layer (*a*) and temperature of its surface (*b*) for steel anode in argon welding: *a* — *1* — j_a = 200; *2* — 500; *3* — 1000 A/cm^2 at T_s = 2472 K; *b* — *1*–*3* — see Figure 3, *a*, but at $T_e^0 = 7 \cdot 10^3$ K

Composition of the near-anode plasma with the convective mode of evaporation of the anode can be calculated using equations (7) through (9), by assuming that $n_{g0}^0 = n_{g1}^0 = 0$ and supplementing this system of equations with the relationships that determine the concentration and temperature of heavy particles of the expanding vapour near the anode surface. To find the values of $\sum_{Z \ge 0} n_{mZ}^0$ and T_h^0, in this case it is possible to use approximate expressions derived in study [28]:

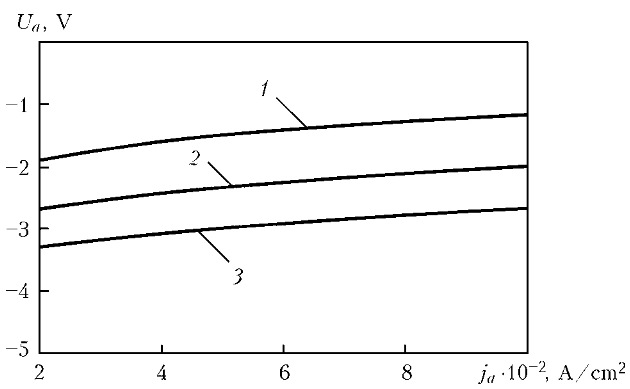

Figure 4. Anode potential drop U_a versus anode current density j_a for steel anode in argon welding (T_s = 2472 K): *1* — $T_e^0 = 6 \cdot 10^3$; *2* — $7 \cdot 10^3$; *3* — $8 \cdot 10^3$ K

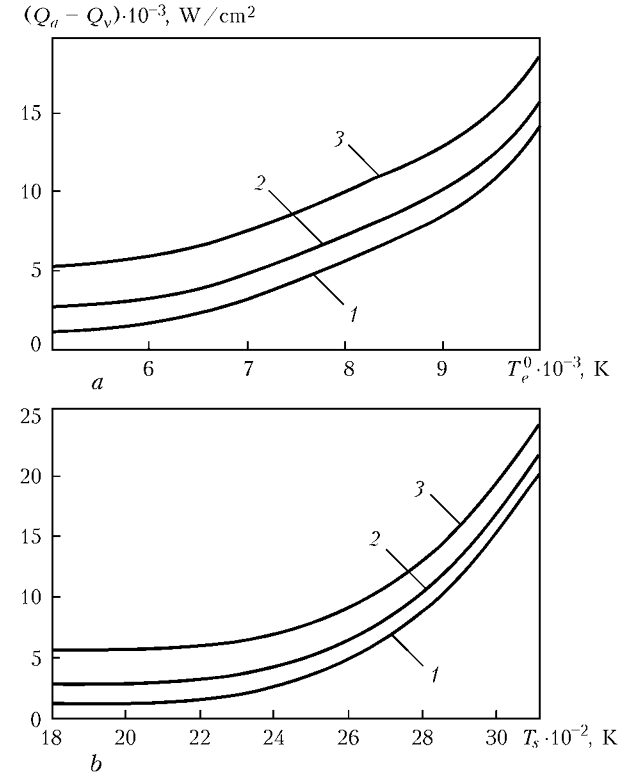

Figure 5. Heat flow on steel anode surface versus electron temperature T_e^0 in the near-anode plasma layer (*a*) and anode surface temperature T_s (*b*) in argon welding: *1–3* — same as in Figure 3

$$\frac{\sum\limits_{Z \ge 0} n^0_{mZ}}{n_s} = \left\{\left(\gamma_m^2 + \frac{1}{2}\right) \exp(\gamma_m^2)\,[1 - \Phi(\gamma_m)] - \frac{\gamma_m}{\sqrt{\pi}}\right\} \times$$

$$\times \sqrt{\frac{T_s}{T_h^0}} + \frac{1}{2}\left\{1 - \gamma_m \sqrt{\pi}\, \exp(\gamma_m^2)\,[1 - \Phi(\gamma_m)]\right\} \frac{T_s}{T_h^0}; \qquad (11)$$

$$\frac{T_h^0}{T_s} = 1 + \frac{\gamma_m^2 \pi}{32}\left(1 - \sqrt{1 + \frac{64}{\gamma_m^2 \pi}}\right).$$

Here $n_s = p_s/kT_s$ is the concentration of the saturated vapour corresponding to a given temperature of the anode surface; $\gamma_m = w^0 \left(\frac{M_m}{2kT_h^0}\right)^{1/2}$ is the dimensionless vapour velocity; and $\Phi(\gamma_m)$ is the probability integral.

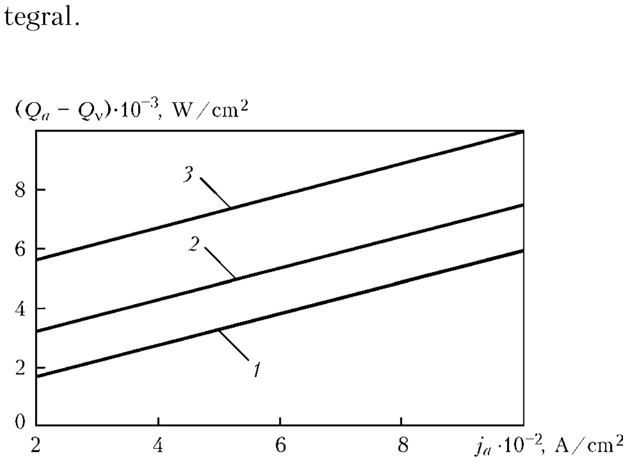

Figure 6. Heat flow to the steel anode surface versus current density j_a in it in argon welding, T_s = 2472 K: *1–3* — see Figure 3

Note that velocity w^0 is an external parameter, and it is determined by conditions of expansion of the vapour in the gas-dynamic region (arc column). To numerically estimate the w^0 value in a case of the subsonic plasma flow, it is possible to use the following approximate expression [28]:

$$w^0 = s^0 \left(\frac{p_m^0}{p^0} - 1\right) \Big/ \gamma^0 \sqrt{1 + \frac{\gamma^0 + 1}{2\gamma^0}\left(\frac{p_m^0}{p^0} - 1\right)}, \qquad (12)$$

where s^0 is the local sound velocity, and γ^0 is the adiabatic exponent for the shielding or plasma gas under normal conditions.

The values of the anode potential drop calculated in this way for the conditions characteristic of TIG welding of steel in argon atmosphere are shown in Figure 3. As follows from the calculation data, the anode potential drop in the system under consideration is negative, increasing in its absolute value with growth of the electron temperature of the plasma near the anode and temperature of its surface (see Figure 3), and decreasing to some extent with increase in the anode current density (Figure 4). The U_a value under the conditions considered is within a range of −1 to −4 V.

Consider now the energy transfer processes occurring in the anode region of the electric arc. Heat flow Q_a from the near-anode plasma to the anode surface has the following form:

$$Q_a = Q_e + Q_i, \qquad (13)$$

where Q_e and Q_i are the flows of the potential and kinetic energy transferred with electrons and ions, respectively.

Write down the expression for Q_e in the following form [24]:

$$Q_e = j_e \left(\frac{5kT_e^0}{2e} + \varphi_m\right), \qquad (14)$$

where φ_m is the work function of electrons for a given metal.

Allowing for the initial energy of ions at the external boundary of the space charge layer, as well as for their extra acceleration in this layer, it can be written down for Q_i

$$Q_i = \sum_{\alpha = m,\, g;\, Z \ge 0} j_{\alpha Z} \left(\overline{\varphi} + \frac{M_\alpha \overline{V_i^2}}{2e} + \frac{1}{Z}\sum_{Z'=1}^{Z} U_{\alpha Z'} - \varphi_m\right), \qquad (15)$$

where $\overline{\varphi} \equiv \varphi(\overline{x}) = \varphi^0 - \frac{1}{2}\frac{kT_e^0}{e}$ is the plasma potential at the boundary of the space charge layer

$$\overline{\varphi} = \varphi^0 - \frac{T_e^0 (w^0)^2 \sum_{Z \ge 1} M_m n_{mZ}^0}{8e \sum_{Z \ge 1} (Z T_e^0 + T_h^0) n_{mZ}^0} \times$$

$$\times \left\{ 1 + \sqrt{1 + \frac{4 \sum_{Z \ge 1} k(Z T_e^0 + T_h^0) n_{mZ}^0}{(w^0)^2 \sum_{Z \ge 1} M_m n_{mZ}^0}} \right\}^2$$

for the case of the convective evaporation mode)].

Expression (13) can be written down in the following form:

$$Q_a = j_a V_a, \quad (16)$$

where V_a is the voltage equivalent of heat released at the anode, which always takes a positive value, in contrast to anode potential drop U_a. Allowing for (1), (14) and (15), find

$$V_a = \varphi_m + \frac{j_e}{j_a} \frac{5kT_e^0}{2e} + \sum_{\alpha = m,\, g;\, Z \ge 0} \frac{j_{\alpha Z}}{j_a} \left(\overline{\varphi} + \frac{M_\alpha \overline{V_i^2}}{2e} + \frac{1}{Z} \sum_{Z' = 1}^{Z} U_{\alpha, Z'} \right). \quad (17)$$

In the case of the convective mode of evaporation of the anode metal, energy Q_v removed from the melt surface by the metal vapour flow should be taken into account while considering the energy balance on the anode surface

$$Q_v = \sum_{Z \ge 0} n_{mZ}^0 w^0 \lambda_v. \quad (18)$$

As far as the pressure on the molten anode metal (weld pool) surface is concerned, in the diffusion evaporation mode it is equal to the plasma pressure determined by solving the gas-dynamic equations for the arc column, whereas in the convective evaporation mode this pressure, allowing for the reactive component, can be calculated from the following expression [29]:

$$p_s = p_m^0 \left(1 + \frac{5}{3} \mathrm{M}^2 \right), \quad (19)$$

where $\mathrm{M} \equiv w^0 / s^0$ is the value of the Mach number at a boundary between the anode region and arc column.

Figures 5 and 6 show the calculation results for a heat flow to the anode, considering the energy losses for evaporation under conditions characteristic of TIG welding of steel in argon atmosphere. As follows from the given calculation curves, the values of Q_a grow with increase of the electron temperature in the near-anode plasma layer, current density at the anode and temperature of its surface. This trend is most pronounced in dependence $Q_a - Q_v(T_s)$ (see Figure 5).

Model of the arc column. To describe the processes of heat, mass and charge transfer in the gas-dynamic region of the plasma (in the arc column), which contains atoms and ions of the evaporated anode metal along with particles of the shielding or plasma gas, we use the model of the two-temperature ionisation-equilibrium plasma. The corresponding system of equations written down, e.g. in cylindrical coordinates (see Figure 1) has the following form [2]:

- continuity equation

$$\frac{\partial \rho}{\partial t} + \frac{1}{r} \frac{\partial}{\partial r} (r \rho v) + \frac{\partial}{\partial z} (\rho u) = 0, \quad (20)$$

where ρ is the mass density of the plasma; v and u are the radial and axial components, respectively, of the plasma velocity;

- equations of motion

$$\rho \left(\frac{\partial v}{\partial t} + v \frac{\partial v}{\partial r} + u \frac{\partial v}{\partial z} \right) = -\frac{\partial p}{\partial r} - j_z B_\varphi + \frac{2}{r} \frac{\partial}{\partial r} \left(r \eta \frac{\partial v}{\partial r} \right) + \frac{\partial}{\partial z} \left[\eta \left(\frac{\partial u}{\partial r} + \frac{\partial v}{\partial z} \right) \right] - 2\eta \frac{v}{r^2} - \frac{2}{3} \frac{\partial}{\partial r} \left\{ \eta \left[\frac{1}{r} \frac{\partial (r v)}{\partial r} + \frac{\partial u}{\partial z} \right] \right\}; \quad (21)$$

$$\rho \left(\frac{\partial u}{\partial t} + v \frac{\partial u}{\partial r} + u \frac{\partial u}{\partial z} \right) = -\frac{\partial p}{\partial z} + j_r B_\varphi + 2 \frac{\partial}{\partial z} \left(\eta \frac{\partial u}{\partial z} \right) + \frac{1}{r} \frac{\partial}{\partial r} \left[r \eta \left(\frac{\partial u}{\partial r} + \frac{\partial v}{\partial z} \right) \right] - \frac{2}{3} \frac{\partial}{\partial z} \left\{ \eta \left[\frac{1}{r} \frac{\partial (r v)}{\partial r} + \frac{\partial u}{\partial z} \right] \right\}, \quad (22)$$

where j_z and j_r are the axial and radial components, respectively, of the current density in plasma; B_φ is the azimuthal component of the magnetic induction vector; and η is the coefficient of dynamic viscosity of the plasma;

- energy equations

$$n_e C_{pe} \times \left(\frac{\partial T_e}{\partial t} + v \frac{\partial T_e}{\partial r} + u \frac{\partial T_e}{\partial z} \right) = \frac{1}{r} \frac{\partial}{\partial r} \left(r \chi_e \frac{\partial T_e}{\partial r} \right) + \frac{\partial}{\partial z} \left(\chi_e \frac{\partial T_e}{\partial z} \right) + \frac{k}{e} \left\{ j_r \frac{\partial [(5/2 - \delta) T_e]}{\partial r} + j_z \frac{\partial [(5/2 - \delta) T_e]}{\partial z} \right\} + \frac{j_r^2 + j_z^2}{\sigma} - \psi - \beta (T_e - T_h); \quad (23)$$

$$\rho C_p \left(\frac{\partial T_h}{\partial t} + v \frac{\partial T_h}{\partial r} + u \frac{\partial T_h}{\partial z} \right) = \frac{1}{r} \frac{\partial}{\partial r} \left(r \chi \frac{\partial T_h}{\partial r} \right) + \frac{\partial}{\partial z} \left(\chi \frac{\partial T_h}{\partial z} \right) + \beta (T_e + T_h), \quad (24)$$

where C_{pe} is the specific heat of the electron gas, allowing for the ionisation energy; χ_e is the coefficient of electron thermal conductivity; δ is the constant of thermal diffusion of electrons; σ is the specific electrical conductivity of the plasma; ψ are the energy losses for radiation (approximation of the optically thin plasma); β is the coefficient of heat exchange between electrons and heavy particles; C_p is the specific heat of a heavy component of the plasma (atoms and ions); and χ is the coefficient of thermal conductivity of the heavy component;

- electromagnetic field equations

$$\frac{1}{r}\frac{\partial}{\partial r}\left(r\sigma\frac{\partial\varphi}{\partial r}\right)+\frac{\partial}{\partial z}\left(\sigma\frac{\partial\varphi}{\partial z}\right)=0; \tag{25}$$

$$B_\varphi(r, z)=\frac{\mu^0}{r}\int_0^r j_z(\xi, z)\xi d\xi, \tag{26}$$

where μ^0 is the universal magnetic constant;

$$j_r=-\sigma\frac{\partial\varphi}{\partial r};\quad j_z=-\sigma\frac{\partial\varphi}{\partial z}. \tag{27}$$

To close the system of equations (20) through (27), it is necessary to determine dependence of thermal-physical characteristics ρ, C_{pe} and C_e, transfer coefficients η, χ_e, χ, δ and σ, heat transfer coefficient β and radiation losses ψ upon the temperature, pressure and composition of the arc plasma. Composition of the multi-component plasma of the arc column with the evaporating anode can be found using equations (7) through (9), which should be supplemented with the following equation of convective diffusion of the metal vapour in the gas-dynamic region:

$$\begin{aligned}\rho\left(\frac{\partial C_m}{\partial t}+v\frac{\partial C_m}{\partial r}+u\frac{\partial C_m}{\partial z}\right)&=\\=\frac{1}{r}\frac{\partial}{\partial r}\left(r\rho D_{m0}\frac{\partial C_m}{\partial r}\right)&+\frac{\partial}{\partial z}\left(\rho D_{m0}\frac{\partial C_m}{\partial z}\right)+\\+\frac{1}{r}\frac{\partial}{\partial r}\left(r\rho\left[\overline{D}_{m1}\frac{\partial C_{m1}}{\partial r}+\overline{D}_{m2}\frac{\partial C_{m2}}{\partial r}\right]\right)&+\\+\frac{\partial}{\partial z}\left(\rho\left[\overline{D}_{m1}\frac{\partial C_{m1}}{\partial z}+\overline{D}_{m2}\frac{\partial C_{m2}}{\partial z}\right]\right)&.\end{aligned} \tag{28}$$

Here $C_m=\frac{M_m\sum_{Z\geq 0}n_{mZ}}{\rho}$ is the relative mass concentration of the metal vapour in the arc column plasma; $C_{m1}=\frac{M_mn_{m1}}{\rho}$ and $C_{m2}=\frac{M_mn_{m2}}{\rho}$ are the relative mass concentrations of metal ions; $\overline{D}_{m1}=D_{m1}-D_{m0}$, $\overline{D}_{m2}=D_{m2}-D_{m0}$, where D_{m0}, D_{m1} and D_{m2} are the coefficients of diffusion of atoms, single- and double-charged ions in the multi-component plasma. Solution of this equation requires evaluation of dependence of diffusion coefficients D_{m0}, D_{m1} and D_m upon the temperature, pressure and composition of the plasma. It should be noted that equation (28), in contrast to the diffusion equation used in study [11], allows for diffusion of ions of the metal vapour.

To solve the system of differential equations (20) through (25) and (28), it is necessary to specify the corresponding initial and boundary conditions. As physical fields in the arc discharge can be set readily enough, the initial distribution of the velocity and temperature is of no fundamental importance. Zero values can be set for the velocity, and the temperature of electrons in the current channel region should provide the plasma conductivity characteristic of the arc discharge. Standard boundary conditions described in detail, e.g. in [2, 9, 17] can be chosen for the boundaries ($r=0$, $r=R_1$, $z=0$, $z=L_1$) of the calculation region (see Figure 1). It remains to set conditions at the boundary of the anode and gas-dynamic regions of the plasma.

Let Γ be the boundary of the anode region with the arc column (because of a small thickness of the anode region, anode surface $z=L_1$ can be regarded as Γ). Then the boundary conditions for equations (20) through (22) at this boundary can be set as follows:

$$v_t\big|_\Gamma=0;$$

$$v_n\big|_\Gamma=\begin{cases}0 & \text{(diffusion evaporation mode)},\\ w^0 & \text{(convective evaporation mode)}.\end{cases} \tag{29}$$

Here v_t and v_n are the tangential and normal plasma components relative to the anode surface, while to calculate distribution of the w^0 values along the anode surface it is possible to use approximate formula (12). Note that more accurate is to find the w^0 values from equations (11) and condition

$$n_e^0kT_e^0+\sum_{Z\geq 0}n_{mZ}^0kT_h^0-\Delta p=p^0,$$

where p^0 is the distribution of the plasma pressure near the anode along its surface, which is determined by solving the gas-dynamic problem.

Designate the vector of normal to Γ (in a direction of the arc column) as $\vec{n}$. Then the corresponding boundary conditions for equations (23) and (24) can be written down in the following form:

$$\chi_e\frac{\partial T_e}{\partial n}\Big|_\Gamma+\chi\frac{\partial T_h}{\partial n}\Big|_\Gamma+j_a\frac{k}{e}\left(\frac{5}{2}-\delta\right)T_e\Big|_\Gamma=$$
$$=\begin{cases}\varphi^0j_a+Q_a & \text{(diffusion evaporation mode)},\\ \varphi^0j_a+Q_a+\varepsilon_v & \text{(convective evaporation mode)};\end{cases} \tag{30}$$

$$T_h\big|_\Gamma=\begin{cases}T_s & \text{(diffusion evaporation mode)},\\ T_h^0 & \text{(convective evaporation mode)},\end{cases} \tag{31}$$

where ε_v are the energy losses for heating and ionisation of the metal vapour coming to the arc column from the anode surface; T_s is the known distribution of temperature over the anode surface, and distribution of the T_h^0 values at the known distributions of T_s and w^0 can be calculated using the second equation in (11).

As conductivity of the anode metal is much higher, as a rule, than the specific electrical conductivity of the plasma, its surface at a sufficient degree of accuracy can be considered equipotential, by assuming, e.g. that $\varphi_a=0$. Then the condition at a boundary between the arc column and anode region for equation (25) can be set in the following form:

$$\varphi\big|_{\Gamma} = \varphi^0, \qquad (32)$$

where distribution of the φ^0 values along the anode surface can be calculated from (6).

Finally, write down the boundary conditions for equation (28) in the following form:

$$C_m\big|_{\Gamma} = \begin{cases} \dfrac{M_m p_s}{\rho^0 k T_s} & \text{(diffusion evaporation mode)},\\ 1 & \text{(convective evaporation mode)}, \end{cases} \qquad (33)$$

where p_s is the distribution of the saturated gas pressure determined at the known distribution of T_s from formula (10); ρ^0 is the distribution of the mass density of the multi-component arc column plasma along the boundary with the anode region.

This exhausts description of the self-consistent mathematical model of physical processes occurring in the multi-component plasma of the anode region and column of the electric arc with the evaporating anode for tungsten-electrode and plasma welding conditions in inert atmosphere.

Therefore, only the self-consistent mathematical model, which allows for interrelation of all physical phenomena accompanying arcing, provides the adequate description of physical processes in column of the welding arc and its anode region, permitting generation of the reliable data on the arcing conditions. Model of the anode region of the arc is an important structural component of this model, responsible for interaction of thermal and electrical processes in the arc column and at the anode (workpiece). Models of properties of the multi-component plasma of the welding arc (ionisation composition, thermodynamic, transport and optical properties), which are determined depending upon the chemical composition of the shielding gas, content of the evaporated anode metal, plasma temperature and ambient pressure, are an indispensable component of the self-consistent model. The input parameters of the self-consistent model should be a set of technological parameters (welding current, shielding gas composition, arc length, etc.), whereas other distributed and integrated characteristics of the arc should be determined as a result of a calculation experiment on the basis of the said model.

1. Hsu, K.S., Etemadi, K., Pfender, E. (1983) Study of the free-burning high-intensity argon arc. *J. of Appl. Phys.*, 54(**3**), 1293–1301.
2. Hsu, K.S., Pfender, E. (1983) Two-temperature modeling of the free-burning high-intensity arc. *Ibid.*, 54(**8**), 4359–4366.
3. Engelsht, V.S., Gurovich, V.Ts., Desyatkov, G.A. et al. (1990) *Low-temperature plasma*. Vol. 1: Theory of electric arc column. Novosibirsk: Nauka.
4. Zhu, P., Lowke, J.J., Morrow, R. et al. (1995) Prediction of anode temperatures of free burning arcs. *J. Phys. D: Appl. Phys.*, **28**, 1369–1376.
5. Jenista, J., Heberlein, J.V.R., Pfender, E. (1997) Numerical model of the anode region of high-current electric arcs. *IEEE Transact. on Plasma Sci.*, 25(**5**), 883–890.
6. Lowke, J.J., Morrow, R., Haidar, J. (1997) A simplified unified theory of arcs and their electrodes. *J. Phys. D: Appl. Phys.*, **30**, 2033–2042.
7. Haidar, J. (1999) Non-equilibrium modeling of transferred arcs. *Ibid.*, **32**, 263–272.
8. Sansonnets, L., Haidar, J., Lowke, J.J. (2000) Prediction of properties of free burning arcs including effects of ambipolar diffusion. *Ibid.*, **33**, 148–157.
9. Fan, H.G., Kovacevic, R. (2004) A unified model of transport phenomena in gas metal arc welding including electrode, arc plasma and molten pool. *Ibid.*, **37**, 2531–2544.
10. Nishiyama, H., Sawada, T., Takana, H. et al. (2006) Computational simulation of arc melting process with complex interactions. *ISIJ Int.*, 46(**5**), 705–711.
11. Hu, J., Tsai, H.L., (2007) Heat and mass transfer in gas metal arc welding. Pt 1: The arc. *Int. J. of Heat and Mass Transfer*, **50**, 833–846.
12. Masquere, M., Freton, P., Gonzalez, J.J. (2007) Theoretical study in two dimensions of the energy transfer between an electric arc and an anode material. *J. Phys. D: Appl. Phys.*, **40**, 432–446.
13. Li He-Ping, Benilov, M.S. (2007) Effect of a near-cathode sheath on heat transfer in high-pressure arc plasmas. *Ibid.*, 2010–2017.
14. Tanaka, M., Yamamoto, K., Tashiro, S. et al. (2008) Metal vapour behaviour in gas tungsten arc thermal plasma during welding. *Welding in the World*, 52(**11/12**), 82–88.
15. Benilov, M.S. (2008) Understanding and modeling plasma-electrode interaction in high-pressure arc discharges: A review. *J. Phys. D: Appl. Phys.*, **41**, 30.
16. Mojzhes, B.Ya., Nemchinsky, V.A. (1972) To the theory of high-pressure arc at refractory cathode. *Zhurnal Teoret. Fiziki*, 42(**5**), 1001–1009.
17. Mojzhes, B.Ya., Nemchinsky, V.A. (1973) To the theory of high-pressure arc at refractory cathode. Pt 2. *Ibid.*, 43(**11**), 2309–2317.
18. Zhukov, M.F., Kozlov, N.P., Pustogarov, A.V. et al. (1982) *Near-electrode processes in arc discharges*. Novosibirsk: Nauka.
19. Wendelstorf, J., Simon, G., Decker, I. et al. (1997) Investigation of cathode spot behaviour of atmospheric argon arcs by mathematical modeling. In: *Proc. of 12th Int. Conf. on Gas Discharges and Their Applications* (Germany, Greifswald, 1997). Vol. 1, 62–65.
20. Nemchinsky, V.A., Perets, L.N. (1977) Near-anode layer of high-pressure high-current arc. *Zhurnal Teoret. Fiziki*, 47(**9**), 1868–1875.
21. Dinulescu, H.A., Pfender, E. (1980) Analysis of the anode boundary layer of high intensity arcs. *J. of Appl. Phys.*, 51(**6**), 3149–3157.
22. Krivtsun, I.V. (2001) Model of evaporation of metal in arc, laser and laser-arc welding. *The Paton Welding J.*, **3**, 2–9.
23. Dyuzhev, G.A., Nemchinsky, V.A., Shkolnik, S.M. et al. (1983) Anode processes in high-current arc discharge. *Khimiya Plazmy*, **10**, 169–209.
24. Sanders, N.A., Pfender, E. (1984) Measurement of anode falls and anode heat transfer in atmospheric pressure high intensity arcs. *J. of Appl. Phys.*, 55(**3**), 714–722.
25. Baksht, F.G., Dyuzhev, G.A., Mitrofanov, N.K. et al. (1973) Probe measurements in low-temperature dense plasma at high ionization degrees. *Zhurnal Teoret. Fiziki*, 43(**12**), 2574–2583.
26. Chen, F. (1967) Electric probes. In: *Diagnostics of plasma*. Moscow: Mir.
27. Griem, H.R. (1962) High-density correction in plasma spectroscopy. *Phys. Rev.*, **128**, 997–1001.
28. Knight, Ch.J. (1979) Theoretical modeling of rapid surface vaporization with back pressure. *AIAA J.*, 17(**5**), 519–523.
29. Arutyunyan, R.V., Baranov, V.Yu., Bolshov, L.A. et al. (1989) *Effect of laser radiation on materials*. Moscow: Nauka.